

What Matters for Grocery Product Retrieval with Open Source Vision Language Models

Emmanuel G. Maminta¹ and Rowel O. Atienza^{1,2}

¹ AI Graduate Program, University of the Philippines, Diliman, Quezon City

² EEEI, University of the Philippines, Diliman, Quezon City
emmanuel.maminta@eee.upd.edu.ph, rowel@eee.upd.edu.ph

Abstract. Multimodal product retrieval (MPR) underpins checkout-free retail and automated inventory systems, yet it demands fine-grained SKU discrimination that standard vision-language benchmarks fail to capture. We present the first systematic zero-shot evaluation of 190 open-source VLMs on the MPR task of the GroceryVision Challenge, isolating pre-training data, architecture, and input resolution. Our analysis yields three actionable findings. **(1) Data quality trumps scale.** Switching from raw web-scrapes to filtered datasets delivers up to 16.6% accuracy gains, exceeding the benefit of doubling model parameters. **(2) Efficient models can win.** MobileCLIP-B (150M parameters) outperforms 351M counterparts trained on noisy data. We introduce *semantic power density* (ϕ), an efficiency metric that penalizes sub-threshold accuracy. **(3) A precision gap persists.** State-of-the-art models achieve 94.5% Recall@5 but suffer a 17.5% drop at Recall@1, revealing that contrastive embeddings cluster categories effectively but fail to rank visually similar SKUs. Code and evaluation scripts are available at <https://github.com/upeee/openmpr>.

Keywords: Multimodal product retrieval · VLMs · Retail intelligence.

1 Introduction

Visual recognition of packaged goods is the cornerstone of modern retail intelligence, enabling checkout-free stores and automated supply chain management. Historically, this task relied on manual feature extraction before evolving into deep learning models trained for closed-set classification. However, new SKUs and packaging redesigns appear daily, making fixed classifiers operationally unsustainable.

To address this rigidity, the paradigm has shifted toward Multimodal Product Retrieval (MPR) using foundation Vision Language Models (VLMs) such as CLIP [26]. As illustrated in Fig. 1, MPR frames recognition as a dynamic ranking task where each probe image is matched against a textual catalog via cross-modal similarity. This approach theoretically enables zero-shot classification but introduces model selection ambiguity. Standard benchmarks like ImageNet prioritize coarse semantic categorization, while retail applications demand fine-grained instance discrimination to separate nearly identical SKUs. Prior works

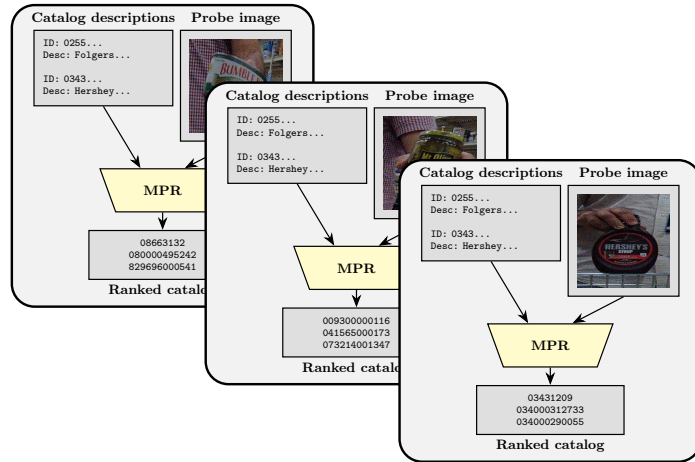


Fig. 1. The MPR inference protocol. MPR frames recognition as a ranking task. For each probe image, cross-modal similarity sorts SKUs by relevance, enabling zero-shot identification.

have fine-tuned VLMs for retail domains [29] or evaluated specific architectures [6], but no systematic zero-shot benchmark isolates the effects of pre-training data, architecture, and input resolution.

To bridge this gap, we conduct a systematic evaluation of 190 open-source models from the OpenCLIP [14] repository on the 4th GroceryVision Challenge [9]. We included all dual-encoder checkpoints available as of September 2025, excluding only corrupted weights. Our findings are specific to grocery products, where inter-SKU visual similarity is high; generalization to fashion, electronics, and other retail domains is an open question. Unlike previous studies that conflate multiple variables, we strictly control for architecture, dataset source, and input resolution. Our contributions are:

1. **Data quality trumps scale.** Dataset filtration predicts zero-shot MPR performance better than parameter count. Switching from raw web-scrapes to filtered sources yields up to a 16.6% accuracy gain, more than doubling the model size would deliver.
2. **Scaling anomalies favor efficient models.** We identify cases where compact models outperform larger baselines. MobileCLIP-B [35] (150M parameters) surpasses 351M counterparts trained on unfiltered data. To quantify this, we propose *semantic power density* (ϕ), an efficiency metric that penalizes poor accuracy-to-parameter ratios.
3. **A systematic ranking precision gap.** We report that models achieve high Recall@5 (94.5%) but suffer a 17.5% drop at Recall@1, indicating that contrastive pre-training produces embeddings suited for coarse retrieval but geometrically unstable for fine-grained ranking.

2 Related Work

Product recognition in retail. Retail product recognition evolved from manual descriptors like SIFT [21] and BRISK [16] to fine-tuned CNNs [28, 25]. Retraining backbones for dynamic catalogs proved prohibitive. GAN-based domain adaptation [33] remains bound by closed-set classification rigidity.

Vision-language models and benchmarks. Foundation models like CLIP [26] established shared embedding spaces enabling open-set retrieval without task-specific training. ELEVATER [17] assesses zero-shot performance across 20 image classification datasets, while DataComp [10] focuses on data-centric evaluation. For fine-grained domains, Products-10K [1], RP2K [25], and GroceryVision [9] provide SKU-level benchmarks. Our work systematically evaluates zero-shot MPR, isolating pre-training data from architecture.

Efficiency metrics and deployment. FLOPs and parameter counts remain standard efficiency proxies but fail to capture task-specific utility. Dehghani et al. [7] show that single cost indicators can mislead and recommend reporting multiple, while scaling-law studies [13] characterize compute-optimal model and data scaling. RetailKLIP [29] fine-tunes a CLIP backbone for retail recognition, and Czerwinska et al. [6] benchmark fine-tuning strategies for e-commerce embeddings. Our semantic power density (ϕ) introduces a deployment-aware metric penalizing models below functional thresholds.

3 Preliminaries

We define the contrastive loss and ranking metrics used in this benchmark.

3.1 Contrastive Representation Learning

We evaluate architectures trained on the CLIP objective, which replaces fixed-label classification with contrastive alignment via InfoNCE loss [24]. The objective maximizes dot-product similarity of B matched image-text pairs $\{(v_i, t_i)\}_{i=1}^B$ while suppressing the $B^2 - B$ in-batch negatives. The symmetric loss \mathcal{L} averages image-to-text and text-to-image components.

$$\mathcal{L}_{I2T} = -\frac{1}{B} \sum_{i=1}^B \log \frac{e^{s(v_i, t_i)/\tau}}{\sum_{j=1}^B e^{s(v_i, t_j)/\tau}} \quad (1)$$

$$\mathcal{L}_{T2I} = -\frac{1}{B} \sum_{i=1}^B \log \frac{e^{s(t_i, v_i)/\tau}}{\sum_{j=1}^B e^{s(t_i, v_j)/\tau}} \quad (2)$$

$$\mathcal{L} = \frac{1}{2}(\mathcal{L}_{I2T} + \mathcal{L}_{T2I}) \quad (3)$$

Here, τ is a learnable temperature controlling distribution sharpness. Lower τ values sharpen the softmax, amplifying gradients from hard negatives. This structures the embedding space such that visual concepts become linearly separable via natural language prompts.

3.2 Problem Formulation and Metric

We treat MPR as a ranking problem. Encoders $f_\theta : \mathcal{V} \rightarrow \mathbb{R}^d$ and $g_\phi : \mathcal{T} \rightarrow \mathbb{R}^d$ map images and text onto a shared hypersphere. Relevance is measured by cosine similarity.

$$s(v, t) = \frac{f_\theta(v) \cdot g_\phi(t)}{\|f_\theta(v)\| \|g_\phi(t)\|} \quad (4)$$

For a given query image v , we maximize the rank of its ground-truth description gt_q . We use the single-gallery-shot protocol where each product has one unique description. The primary metric is Recall@ K (CMC at rank K), measuring the percentage of queries where the correct match appears in the top K results.

$$\text{Recall@}K = \frac{1}{Q} \sum_{q=1}^Q \mathbb{I}(\text{rank}(gt_q) \leq K) \quad (5)$$

4 Benchmark

We detail the catalog metadata refinement and dual-encoder inference protocol.

4.1 MPR Dataset

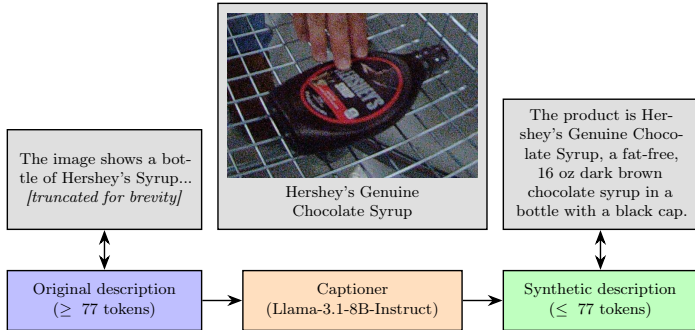


Fig. 2. Caption refinement. Llama-3.1-8B-Instruct compresses descriptions exceeding 77 tokens into concise captions while retaining key visual attributes.

The MPR dataset from the GroceryVision Challenge [9], released under CC-BY-NC 4.0 which permits non-commercial use with attribution, contains 74,200 training images across 409 SKUs, subsampled to 12,944 front-facing perspectives. Original catalog metadata frequently exceeds the 77-token context limit of CLIP text encoders, causing truncation of discriminative attributes. We synthesized concise descriptions using Llama-3.1-8B-Instruct [11]. As shown in Fig. 2, the captioner receives the product description and a tag description emphasizing

visual attributes. Outputs begin with “*The product is...*”, prioritize visual features, and remain within 77 tokens. The prompt template is provided below.

Llama-3.1-8B-Instruct Prompt Template

Role: You are a helpful assistant that generates descriptions for grocery products.

Task: Generate a concise product description in ≤ 77 tokens given the product metadata. Output a JSON object with key “label”.

Constraints:

- Start with “The product is ...” in every description.
- Prioritize prominent visual attributes from the tag description including color, shape, brand, size, packaging, and form.

Generating synthetic descriptions has precedent in retail AI applications [30]. Crucially, we frame this process as semantic restoration rather than augmentation; it recovers ground-truth visual cues lost in truncated metadata to ensure the retrieval target is factually complete. To validate quality, we randomly sampled 250 descriptions (61% of the 409-SKU catalog) and reviewed them in two independent passes using different random seeds. Each description was assessed on a pass/fail basis for token compliance and preservation of key visual attributes (color, shape, brand, size) against source metadata. On this sampled subset we observed 100% token compliance and 100% attribute retention, with no hallucinations identified.

4.2 MPR Pipeline

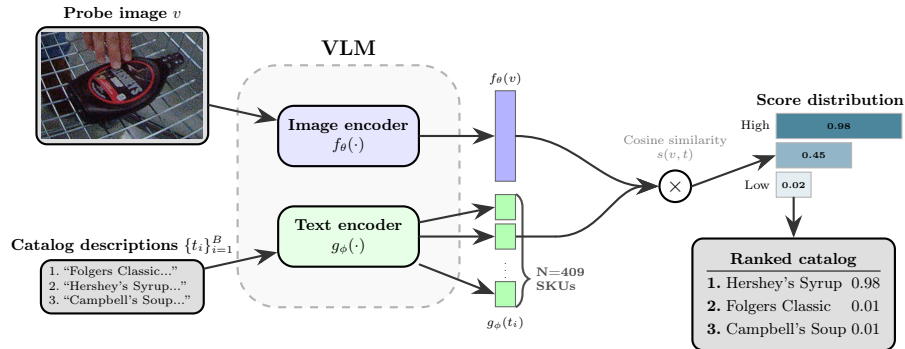


Fig. 3. Architecture of the MPR pipeline. The VLM encoders (f_θ, g_ϕ) map the probe image v and catalog descriptions $\{t_i\}$ into a shared embedding space. We compute the cosine similarity $s(v, t)$ to rank the 409 SKUs.

As illustrated in Figure 3, the pipeline follows a dual-encoder architecture. The system takes a probe image v and $N = 409$ catalog descriptions $\{t_i\}_{i=1}^N$. OpenCLIP instantiates the encoders with diverse checkpoint weights. The image

encoder f_θ and text encoder g_ϕ produce L_2 -normalized embeddings. Relevance is computed via dot product, using sigmoid for SigLIP [39, 34] or softmax for CLIP. All evaluations run on a single A100 (40GB) using `bf16` precision.

5 Analysis

We evaluate 190 models to isolate the drivers of retrieval performance.

5.1 Strongest Open Source VLM for MPR

Which pre-trained VLM provides the strongest foundation for MPR?

Our benchmarking identifies SigLIP2 [34] as the strongest foundation. ViT-gopt-16-SigLIP2-384 achieves zero-shot Recall@1 of 0.770, outperforming ViT-L-14 [26] by 35%. All metrics are computed on the full test set with deterministic inference. We verified stability by running three independent forward passes with different batch orderings, observing standard deviations below 0.002 for all Recall@ K values. Table 1 shows modern SigLIP variants dominate the leaderboard. However, state-of-the-art (SOTA) retrieval requires 1.8B parameters. PE-Core [2] achieves 0.758 with only 671M parameters, offering near-peak performance at one-third the cost.

Table 1. SOTA hierarchy for MPR. SigLIP2 models establish a new MPR baseline. PE-Core achieves 98% of peak accuracy at one-third the parameters.

Checkpoint	Size (M)	PT data	Recall@1
ViT-gopt-16-SigLIP2-384 [34]	1871	WebLI-10B [4]	0.770
PE-Core-L-14-336 [2]	671	MetaCLIP-5.4B [37]	0.758
ViT-SO400M-14-SigLIP2-378 [34]	1136	WebLI-10B [4]	0.749
ViT-L-16-SigLIP2-384 [34]	882	WebLI-10B [4]	0.701
ViT-L-14 [26]	428	WIT-400M [26]	0.568

Our analysis uncovers a non-linear relationship between resolution and accuracy. Table 2 shows ViT-L-16-SigLIP2 peaks at 384px and plateaus at 512px. ViTamin-XL [3] peaks at 256px with sharp drops at 384px. We hypothesize that beyond optimal resolution, ViTs [8] over-index on high-frequency noise such as JPEG artifacts and sensor noise. Table 2 bears this out: compute grows quadratically while accuracy plateaus or regresses. We conclude 384px is the practical ceiling for MPR.

What is the best model for a specific memory budget? Table 3 shows top models per parameter class. MobileCLIP-B achieves 0.653 Recall@1 despite having half the parameters of ConvNeXt-Large-d-320 [20] at 0.645. The DataCompDR [35] distillation process explains this. ConvNeXt learns from LAION-2B [27], a web-scraped dataset with substantial noise from misaligned image-text pairs [10].

Table 2. The resolution wall. Performance plateaus or regresses beyond 384px. Compute cost grows quadratically while accuracy degrades. 384px is the practical efficiency ceiling for MPR.

Architecture (Comparison)	Low res. (Recall@1)	High res. (Recall@1)	Delta (Accuracy)	Compute cost (FLOPs)
ViT-L-16-SigLIP2 [34]	0.701 (384px)	0.700 (512px)	-0.1%	+1.7×
ViTamin-XL [3]	0.687 (256px)	0.670 (384px)	-2.5%	+2.2×
ViT-L-14 [26]	0.568 (224px)	0.561 (336px)	-1.2%	+2.2×

MobileCLIP trains on synthetic captions and embeddings distilled from a teacher ensemble pre-trained on filtered data. We did not measure inference latency directly. The ϕ metric serves as a theoretical guide but practitioners should validate on target hardware. MobileCLIP-B is optimal for 150M budget on-device applications. PE-Core-L-14 delivers 98.4% of peak at one-third compute for server-side deployment.

Table 3. Size class leaders. MobileCLIP-B outperforms larger models through knowledge distillation. Data quality matters more than parameter count for edge deployment. PT: Pre-training.

Size family	Checkpoint	PT data	Size	Recall@1
Small (< 200M)	MobileCLIP-B [35]	DataCompDR [35]	150M	0.653
Medium (200–400M)	ConvNeXt-Large-d-320 [20]	LAION-2B [27]	351M	0.645
Large (400M–1B)	PE-Core-L-14-336 [2]	MetaCLIP [37]	671M	0.758
Very Large (> 1B)	ViT-gopt-16-SigLIP2-384 [34]	WebLI [4]	1.8B	0.770

5.2 Influence of Pre-training Data on Downstream MPR

What influence do pre-training datasets have on MPR? Dataset filtration quality determines zero-shot transfer more than model scale. We observe a strict hierarchy where filtered datasets like DataComp [10] consistently outperform raw LAION [27] and WIT-400M [26] across all architectures. Table 4 shows a monotonic relationship between filtering rigor and Recall@1. The performance gap widens as model capability increases, suggesting higher-capacity models require higher-fidelity signals. Changing data source yields higher return than doubling parameters. Table 5 shows ViT-B-32 suffers 79.4% failure on noisy CommonPool [10] while ViT-L-14 maintains parity. The large model locks onto the dominant clean signal and ignores outliers. Data purity requirements scale inversely with capacity.

Does architecture protect against data scarcity? No. YFCC-15M is a 15-million image subset of YFCC100M [32] comprising user-uploaded Flickr photos with noisy metadata. Table 6 shows ResNet50 [12] and ResNet101 suffer >93%

Table 4. Universal scaling of data quality. We compare Recall@1 of the same architectures pre-trained on different data sources. DataComp-XL (filtered) consistently outperforms LAION-2B (raw scale) and WIT-400M (web scrape), confirming that data quality is a universal efficiency multiplier.

Backbone (size)	WIT-400M [26] (web scrape)	LAION-2B [27] (raw scale)	DataComp-XL [10] (filtered)	Curated gain (Δ vs WIT-400M)
ViT-B-32 (151M) [26]	0.403	0.481	0.521	+11.8%
ViT-B-16 (150M) [26]	0.443	0.535	0.608	+16.6%
ViT-L-14 (428M) [26]	0.568	0.619	0.693	+12.5%

Table 5. Capacity works as a filter. Large models can survive noisy data, while small models collapse. This creates a distillation trap since one cannot simply distill a large, robust model into a small edge model using noisy data. Efficient models require strictly higher-purity data to converge.

Backbone (size)	WIT-400M [26] (baseline)	CommonPool [10] (noisy)	DataComp-XL [10] (filtered)	Noise penalty (CommonPool vs. WIT-400M)
ViT-B-32 (151M) [26]	0.403	0.083	0.521	-79.4% (collapse)
ViT-B-16 (150M) [26]	0.443	0.267	0.608	-39.7% (degraded)
ViT-L-14 (428M) [26]	0.568	0.574	0.693	+1.0% (resilient)

drops from WIT-400M to YFCC-15M. Collapse is universal across architectures. Consequently, our benchmarking identifies a distinct shift in the data frontier. Table 7 confirms SOTA models abandon raw scraping for filtered data.

Table 6. Universal scale sensitivity. We compare identical architectures trained on large-scale web data (WIT-400M) vs. small, uncurated subsets (YFCC/CommonPool). The collapse is universal across depth (ResNet101), architecture (ViT), and activation function (quickgelu), confirming that data scale is a primary driver of zero-shot retrieval capability. PT: Pre-training.

Backbone	Large-scale PT data (400M)	Small-scale PT data (12–15M)	Recall@1 (Large)	Recall@1 (Small)	Collapse ratio
ResNet50 [12]	WIT	YFCC	0.405	0.018	-95.5%
ResNet50-quickgelu [14]	WIT	YFCC	0.386	0.019	-95.1%
ResNet101 [12]	WIT	YFCC	0.438	0.027	-93.8%
ResNet101-quickgelu [14]	WIT	YFCC	0.399	0.025	-93.7%
ViT-B-32 [26]	WIT	CommonPool-S	0.403	0.010	-97.5%

5.3 Quantifying Return on Investment for MPR

Which architecture yields highest ROI? Standard benchmarks plot accuracy linearly against size, but deployment utility follows a sigmoidal curve. Below 50% accuracy, a model returns more false charges than correct retrievals (odds ratio < 1) and cannot operate autonomously. Above 80% accuracy, errors become rare

Table 7. Dataset leaders. The top performers all abandon raw scraping. Aggressive filtering or WebLI signals yield the best results.

Data	Methodology	Checkpoint	Recall@1
WebLI [4]	Image-text similarity filtering	ViT-gopt-16-SigLIP2-384 [34]	0.770
DataComp-1B [10]	Similarity filtering	ViTamin-L2-384 [3]	0.697
DataCompDR [35]	Multi-modal reinforcement	MobileCLIP-B [35]	0.653
LAION-2B [27]	Raw scaling	ViT-L-14-laion2b_s32b_b82k [14]	0.619

enough to tolerate (odds ratio ≥ 4). We therefore anchor our efficiency metric at 50%, the minimum viability threshold where the odds ratio crosses 1. This utility profile motivates a metric that penalizes sub-threshold models instead of linearly rewarding parameter efficiency. We propose semantic power density (ϕ) (Eq. 6). Drawing from signal processing, we treat the retrieval odds ratio as the signal amplitude, setting $\epsilon = 10^{-6}$. Since effective power scales with the square of the amplitude ($P \propto A^2$), we define the metric as the squared Signal-to-Noise Ratio (SNR) normalized by number of parameters in millions:

$$\phi = \frac{\left(\frac{\text{Recall@1}}{1-\text{Recall@1}+\epsilon}\right)^2}{N_{\text{params}}} \times 100 \quad (6)$$

Table 8. Comparison of efficiency metrics. We evaluate three formulations on representative models. The linear metric (M_1) incorrectly favors small but inaccurate models. The quadratic-accuracy metric (M_2) improves ordering but lacks a principled threshold. Our SNR-based ϕ correctly identifies MobileCLIP-B as optimal by severely penalizing sub-50% models.

Model	Size (M)	Recall@1	M_1	M_2	ϕ
			($R@1/N$)	($R@1^2/N$)	(SNR^2/N)
ViTamin-S [3]	62	0.432	0.70	0.30	0.93
ResNet50 [12]	102	0.405	0.40	0.16	0.45
MobileCLIP-B [35]	150	0.653	0.44	0.28	2.37
ViT-L-14 [26]	428	0.568	0.13	0.08	0.41
PE-Core-L-14 [2]	671	0.758	0.11	0.09	1.46
<i>Correct ranking?</i>			✗	Partial	✓

Why SNR? Table 8 shows linear metrics rank ViTamin-S [3] (62M, 43.2%) above MobileCLIP-B [35] (150M, 65.3%). Our SNR-based ϕ creates a deployment threshold at 50%. This threshold is principled. At 50% accuracy, the odds ratio equals 1, meaning success and failure are equiprobable. Below this, the model produces more errors than correct retrievals. The 50% choice targets autonomous retail systems; applications with cheaper error recovery can re-parameterize ϕ

without changing its SNR structure. Above 50%, signal power grows super-linearly, filtering out functionally obsolete architectures (Fig. 4). For edge deployment, we propose prioritizing candidates with high Recall@ K , then validating ϕ . If a model relies on Recall@5 for coverage, a lightweight reranker bridges the accuracy gap.

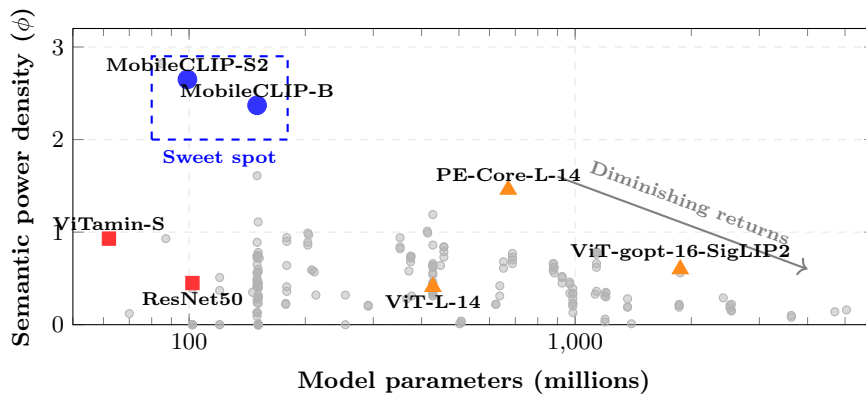


Fig. 4. The edge-centric efficiency landscape. Semantic power density (ϕ) vs. model size. Gray dots show the full population ($N = 190$). Blue circles mark high-efficiency MobileCLIP models. Red squares indicate poor ROI. Triangles represent massive models with low density due to parameter bloat. MobileCLIP occupies the sweet spot for edge deployment.

Table 9. The efficiency hierarchy. MobileCLIP-S2 generates $3\times$ more signal per parameter than ViTamin-S. Reducing size is a false economy if accuracy drops below usable thresholds. **Bold** is SOTA accuracy. Underline is peak density. Double underline is optimal edge trade-off.

Model checkpoint	Family	Size (M)	Recall@5	Recall@1	ϕ
<i>High density</i>					
MobileCLIP-S2 [35]	MobileCLIP	99	0.835	<u>0.619</u>	<u>2.65</u>
MobileCLIP-B [35]	MobileCLIP	150	0.860	<u>0.653</u>	<u>2.37</u>
<i>Low density</i>					
PE-Core-L-14-336 [2]	PE-Core	671	0.937	0.758	1.46
ViTamin-S [3]	ViTamin	62	0.674	0.432	0.93
ViT-gopt-16-SigLIP2-384 [34]	SigLIP2	1871	0.945	0.770	0.60
ResNet50 [12]	ResNet	102	0.637	0.405	0.45
ViT-L-14 [26]	ViT	428	0.814	0.568	0.41

Table 10. Efficiency breakdown by family. Peak ϕ across 14 architectural families. MobileCLIP establishes the efficiency ceiling ($\phi = 2.82$). Legacy and massive-scale architectures offer the lowest return. PT: Pre-training data.

Family	Count	Max ϕ	Backbone	PT data	Recall@5	Recall@1
<i>Tier 1: Hyper-efficient ($\phi > 2.0$)</i>						
MobileCLIP [35]	4	2.82	MobileCLIP-S1	DataCompDR [35]	0.818	0.608
<i>Tier 2: High utility ($1.0 \leq \phi < 2.0$)</i>						
ViT [26]	80	1.61	ViT-B-16	DataComp-XL [10]	0.816	0.608
PE-Core [2]	5	1.46	PE-Core-L-14-336	MetaCLIP [37]	0.937	0.758
ViT-CLIPA [18]	7	1.01	ViT-L-14-CLIPA	DataComp-1B [10]	0.887	0.671
<i>Tier 3: Moderate density ($0.5 \leq \phi < 1.0$)</i>						
ViT-SigLIP [39]	11	0.99	ViT-B-16-SigLIP	WebLI [4]	0.805	0.587
ConvNeXt [20]	12	0.94	ConvNeXt-Base-w	LAION-2B [27]	0.773	0.565
ViTamin [3]	15	0.93	ViTamin-S	DataComp-1B [10]	0.674	0.432
ViT-SigLIP2 [34]	15	0.79	ViT-SO400M-14-SigLIP2-378	WebLI [4]	0.923	0.749
EVA [31]	7	0.64	EVA02-L-14	Merged-2B [31]	0.859	0.624
ResNet [12]	16	0.51	ResNet101	WIT-400M [26]	0.684	0.438
<i>Tier 4: Low density or diminishing returns ($\phi < 0.5$)</i>						
CoCa [38]	4	0.42	CoCa-ViT-L-14	LAION-2B [27]	0.822	0.621
Roberta-ViT [19, 26]	3	0.32	RoBERTa-ViT-B-32	LAION-2B [27]	0.701	0.453
ViT-Worldwide [5]	5	0.22	ViT-H-14	Worldwide [5]	0.877	0.671
NLLB-CLIP [36]	6	0.06	NLLB-Large-SigLIP	NLLB-v1 [36]	0.714	0.453

As shown in Table 9, ϕ aligns strictly with deployment reality. MobileCLIP-S2 dominates the frontier, generating the highest discriminative signal per unit of hardware. This metric solves the monotonicity problem in linear metrics. ViTamin-S ranks in the low-density tier despite its small size, confirming that parameter savings are outweighed by retrieval failures. The metric also highlights the exponential cost of SOTA. ViT-gopt-16-SigLIP2-384 scores only 0.60, demonstrating that while it provides highest absolute fidelity, its power-to-weight ratio is significantly lower than MobileCLIP variants. Table 10 provides a concise overview of the efficiency landscape aggregated by architectural family.

5.4 Retrieval Performance and the Discriminative Gap

We evaluate retrieval using Recall@ K . Table 11 shows ViT-gopt-16-SigLIP2-384 retrieves the correct product within top-5 candidates 94.5% of the time but fails to rank it first in 17.5% of cases. Current VLMs operate as category-level retrievers rather than SKU-level rankers. Pre-training on broad alt-text pushes models to ignore subtle details. The result is high Recall@5 but locally degenerate manifold geometry (Fig. 5 shows a representative confusion case). Embeddings of distinct SKU variants collapse into a narrow cone around their shared visual attributes. The bottleneck is no longer representational capacity but the ranking mechanism itself.

Our analysis points to a two-stage architecture consisting of a frozen VLM retriever followed by a lightweight reranker. Two-stage and late-interaction ranking are standard in information retrieval [23, 15], and the 17.5% gap between Recall@5 and Recall@1 quantifies the available headroom. Since the correct SKU

is already in the top-5 shortlist 94.5% of the time, the remaining task is ranking candidates rather than learning representations. Candidate approaches include cross-attention modules on top- K candidates, pairwise ranking transformers, or a compact VLM repurposed for reranking, such as SmolVLM [22].

Table 11. The discriminative gap. Top models ranked by Recall@5. The gap $\Delta = \text{Recall@5} - \text{Recall@1}$ quantifies precision drop. VLMs excel at narrowing the search space ($\text{Recall@5} \approx 94\%$) but struggle to rank final candidates, with gaps exceeding 17%.

Model checkpoint	Size (B)	Recall@5	Recall@3	Recall@1	Δ
ViT-gopt-16-SigLIP2-384 [34]	1.87	0.945	0.923	0.770	0.175
ViT-gopt-16-SigLIP2-256 [34]	1.87	0.945	0.923	0.763	0.182
PE-Core-L-14-336 [2]	0.67	0.937	0.916	0.758	0.179
PE-Core-bigG-14-448 [2]	2.42	0.933	0.900	0.725	0.208
EVA02-E-14 [31]	4.70	0.929	0.902	0.722	0.207

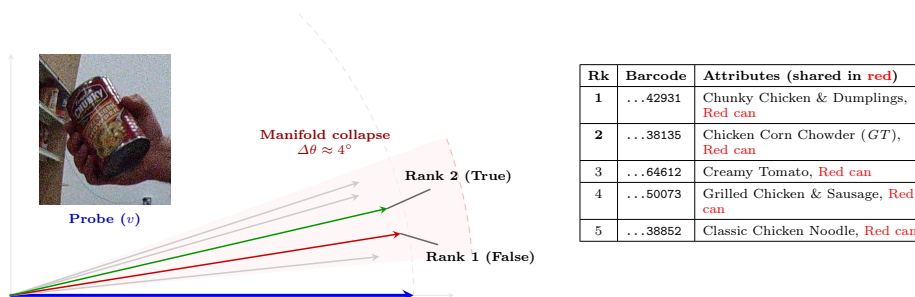


Fig. 5. Manifold collapse illustrated. Embedding projection for a representative query. The model must distinguish *Chicken Corn Chowder* from *Chicken & Dumplings*. Shared visual attributes (red) cause vectors to collapse into a narrow cone of confusion ($\Delta\theta \approx 4^\circ$). Dot product cannot separate them.

6 Conclusion

Our benchmark of 190 VLMs is a diagnostic study of multimodal product retrieval. Three findings challenge prevailing assumptions: (i) data quality, not parameter count, determines the zero-shot ceiling (up to 16.6% gains from filtered sources); (ii) compact models trained on clean data beat noisier larger baselines (MobileCLIP-B at 150M surpasses 351M competitors); (iii) a 17.5% Recall@5-to-Recall@1 gap shows current VLMs discriminate coarse categories but not

SKU-level variants. For deployment, we recommend MobileCLIP-B on edge ($\phi = 2.37$), PE-Core-L-14 on server, and 384px as a practical resolution ceiling.

Limitations. Our evaluation is confined to the GroceryVision dataset (409 SKUs, 74,200 images), a smaller catalog than Products-10K ($\sim 10\text{K}$ products) [1] or RP2K ($\sim 2\text{K}$ products) [25]. Fashion retrieval may call for different resolution ceilings since texture and color demand higher fidelity. Electronics packaging often contains dense text where OCR-augmented models may outperform pure VLMs; we do not claim the 384px ceiling applies universally. We study frozen backbones; fine-tuning and instruction-tuned retrievers are a natural next step.

Future work. The 17.5% gap between Recall@5 and Recall@1 directly motivates a two-stage retrieval follow-up: a lightweight cross-attention or pairwise-ranking reranker over top- K candidates, evaluated to see whether patch-level ViT features retain the discriminative signal that pooled contrastive embeddings throw away. Extensions to multilingual catalogs, non-grocery retail domains, and dynamic inventory settings are natural next steps.

Acknowledgements We thank the GroceryVision 2025 Challenge organizers for the dataset and the University of the Philippines Diliman for providing the computing resources.

References

1. Bai, Y., Chen, Y., Yu, W., Wang, L., Zhang, W.: Products-10k: A large-scale product recognition dataset. arXiv preprint arXiv:2008.10545 (2020)
2. Bolya, D., Huang, P.Y., Sun, P., Cho, J.H., Madotto, A., Wei, C., Ma, T., Zhi, J., Rajasegaran, J., Bangalath, H., Wang, J., Monteiro, M., Xu, H., Dong, S., Ravi, N., Li, S.W., Dollar, P., Feichtenhofer, C.: Perception encoder: The best visual embeddings are not at the output of the network. In: Belgrave, D., Zhang, C., Lin, H., Pascanu, R., Koniusz, P., Ghassemi, M., Chen, N. (eds.) Advances in Neural Information Processing Systems. vol. 38, pp. 60884–60937. Curran Associates, Inc. (2025)
3. Chen, J., Yu, Q., Shen, X., Yuille, A., Chen, L.C.: Vitamin: Designing scalable vision models in the vision-language era. In: Proceedings of the IEEE/CVF conference on computer vision and pattern recognition. pp. 12954–12966 (2024)
4. Chen, X., Wang, X., Changpinyo, S., Piergiovanni, A., Padlewski, P., Salz, D., Goodman, S., Grycner, A., Mustafa, B., Beyer, L., et al.: Pali: A jointly-scaled multilingual language-image model. In: International Conference on Learning Representations (ICLR) (2023)
5. Chuang, Y.S., Li, Y., Wang, D., Yeh, C.F., Lyu, K., Raghavendra, R., Glass, J., Huang, L., Weston, J., Zettlemoyer, L., et al.: Meta clip 2: A worldwide scaling recipe. Advances in Neural Information Processing Systems **38**, 48009–48036 (2026)
6. Czerwinska, U., Bircanoglu, C., Chamoux, J.: Benchmarking image embeddings for e-commerce: Evaluating off-the shelf foundation models, fine-tuning strategies and practical trade-offs. arXiv preprint arXiv:2504.07567 (2025)

7. Dehghani, M., Tay, Y., Arnab, A., Beyer, L., Vaswani, A.: The efficiency misnomer. In: International Conference on Learning Representations (2022)
8. Dosovitskiy, A., Beyer, L., Kolesnikov, A., Weissenborn, D., Zhai, X., Unterthiner, T., Dehghani, M., Minderer, M., Heigold, G., Gelly, S., Uszkoreit, J., Houlsby, N.: An image is worth 16x16 words: Transformers for image recognition at scale. In: International Conference on Learning Representations (2021)
9. Fan, Q., Li, W., Miao, S., Ma, S.: The 4th groceryvision challenge: Iccv25 retailvision workshop. https://grocery-vision.github.io/past_challenge/iccv2025.html (2025), accessed: 2025-11-27
10. Gadre, S.Y., Ilharco, G., Fang, A., Hayase, J., Smyrnis, G., Nguyen, T., Marten, R., Wortsman, M., Ghosh, D., Zhang, J., et al.: Datacomp: In search of the next generation of multimodal datasets. *Advances in Neural Information Processing Systems* **36**, 27092–27112 (2023)
11. Grattafiori, A., et al.: The llama 3 herd of models (2024), <https://arxiv.org/abs/2407.21783>
12. He, K., Zhang, X., Ren, S., Sun, J.: Deep residual learning for image recognition. In: Proceedings of the IEEE conference on computer vision and pattern recognition (CVPR). pp. 770–778 (2016)
13. Hoffmann, J., Borgeaud, S., Mensch, A., Buchatskaya, E., Cai, T., Rutherford, E., de Las Casas, D., Hendricks, L.A., Welbl, J., Clark, A., et al.: Training compute-optimal large language models. In: Proceedings of the 36th International Conference on Neural Information Processing Systems. pp. 30016–30030 (2022)
14. Ilharco, G., Wortsman, M., Wightman, R., Gordon, C., Carlini, N., Taori, R., Dave, A., Shankar, V., Namkoong, H., Miller, J., Hajishirzi, H., Farhadi, A., Schmidt, L.: Openclip (Jul 2021). <https://doi.org/10.5281/zenodo.5143773>, <https://doi.org/10.5281/zenodo.5143773>
15. Khattab, O., Zaharia, M.: ColBERT: Efficient and effective passage search via contextualized late interaction over BERT. In: Proceedings of the 43rd International ACM SIGIR Conference on Research and Development in Information Retrieval. pp. 39–48 (2020)
16. Leutenegger, S., Chli, M., Siegwart, R.Y.: Brisk: Binary robust invariant scalable keypoints. In: 2011 International conference on computer vision. pp. 2548–2555. IEEE (2011)
17. Li, C., Liu, H., Li, L., Zhang, P., Aneja, J., Yang, J., Jin, P., Hu, H., Liu, Z., Lee, Y.J., et al.: Elevater: A benchmark and toolkit for evaluating language-augmented visual models. *Advances in Neural Information Processing Systems* **35**, 9287–9301 (2022)
18. Li, X., Wang, Z., Xie, C.: An inverse scaling law for clip training. *Advances in Neural Information Processing Systems* **36**, 49068–49087 (2023)
19. Liu, Y., Ott, M., Goyal, N., Du, J., Joshi, M., Chen, D., Levy, O., Lewis, M., Zettlemoyer, L., Stoyanov, V.: Roberta: A robustly optimized bert pretraining approach. arXiv preprint arXiv:1907.11692 (2019)
20. Liu, Z., Mao, H., Wu, C.Y., Feichtenhofer, C., Darrell, T., Xie, S.: A convnet for the 2020s. In: Proceedings of the IEEE/CVF conference on computer vision and pattern recognition. pp. 11976–11986 (2022)
21. Lowe, D.G.: Distinctive image features from scale-invariant keypoints. *International journal of computer vision* **60**(2), 91–110 (2004)
22. Marafioti, A., Zohar, O., Farré, M., Noyan, M., Bakouch, E., Cuenca, P., Zakka, C., Allal, L.B., Lozhkov, A., Tazi, N., et al.: Smolvlm: Redefining small and efficient multimodal models. arXiv preprint arXiv:2504.05299 (2025)

23. Nogueira, R., Cho, K.: Passage re-ranking with BERT. arXiv preprint arXiv:1901.04085 (2019)
24. Oord, A.v.d., Li, Y., Vinyals, O.: Representation learning with contrastive predictive coding. arXiv preprint arXiv:1807.03748 (2018)
25. Peng, J., Xiao, C., Li, Y.: Rp2k: A large-scale retail product dataset for fine-grained image classification. arXiv preprint arXiv:2006.12634 (2020)
26. Radford, A., Kim, J.W., Hallacy, C., Ramesh, A., Goh, G., Agarwal, S., Sastry, G., Askell, A., Mishkin, P., Clark, J., et al.: Learning transferable visual models from natural language supervision. In: International conference on machine learning. pp. 8748–8763. PMLR (2021)
27. Schuhmann, C., Beaumont, R., Vencu, R., Gordon, C., Wightman, R., Cherti, M., Coombes, T., Katta, A., Mullis, C., Wortsman, M., et al.: Laion-5b: An open large-scale dataset for training next generation image-text models. *Advances in neural information processing systems* **35**, 25278–25294 (2022)
28. Srivastava, M.M.: Bag of tricks for retail product image classification. In: International Conference on Image Analysis and Recognition. pp. 71–82. Springer (2020)
29. Srivastava, M.M.: Retailclip: Finetuning openclip backbone using metric learning on a single gpu for zero-shot retail product image classification. arXiv preprint arXiv:2312.10282 (2023)
30. Srivastava, S., Wu, K.: Sgbd: Sharpness-aware mirror gradient with blip-based denoising for robust multimodal product recommendation. In: Proceedings of the IEEE/CVF International Conference on Computer Vision (ICCV) Workshops. pp. 2380–2389 (2025)
31. Sun, Q., Fang, Y., Wu, L., Wang, X., Cao, Y.: Eva-clip: Improved training techniques for clip at scale. arXiv preprint arXiv:2303.15389 (2023)
32. Thomee, B., Shamma, D.A., Friedland, G., Elizalde, B., Ni, K., Poland, D., Borth, D., Li, L.J.: Yfcc100m: The new data in multimedia research. *Communications of the ACM* **59**(2), 64–73 (2016)
33. Tonioni, A., Di Stefano, L.: Domain invariant hierarchical embedding for grocery products recognition. *Computer Vision and Image Understanding* **182**, 81–92 (2019)
34. Tschannen, M., Gritsenko, A., Wang, X., Naeem, M.F., Alabdulmohsin, I., Parthasarathy, N., Evans, T., Beyer, L., Xia, Y., Mustafa, B., Hénaff, O., Harmen, J., Steiner, A., Zhai, X.: Siglip 2: Multilingual vision-language encoders with improved semantic understanding, localization, and dense features. arXiv preprint arXiv:2502.14786 (2025)
35. Vasu, P.K.A., Pouransari, H., Faghri, F., Vemulapalli, R., Tuzel, O.: Mobileclip: Fast image-text models through multi-modal reinforced training. In: Proceedings of the IEEE/CVF Conference on Computer Vision and Pattern Recognition (CVPR). pp. 15963–15974 (2024)
36. Visheratin, A.: Nllb-clip–train performant multilingual image retrieval model on a budget. arXiv preprint arXiv:2309.01859 (2023)
37. Xu, H., Xie, S., Tan, X., Huang, P.Y., Howes, R., Sharma, V., Li, S.W., Ghosh, G., Zettlemoyer, L., Feichtenhofer, C.: Demystifying clip data. In: International Conference on Learning Representations (2024)
38. Yu, J., Wang, Z., Vasudevan, V., Yeung, L., Seyedhosseini, M., Wu, Y.: Coca: Contrastive captioners are image-text foundation models. *Transactions on Machine Learning Research* (2022)
39. Zhai, X., Mustafa, B., Kolesnikov, A., Beyer, L.: Sigmoid loss for language image pre-training. In: Proceedings of the IEEE/CVF international conference on computer vision. pp. 11975–11986 (2023)